Side-Chain Interactions Determine Amyloid Formation by Model Polyglutamine Peptides in Molecular Dynamics Simulations

Alexander J. Marchut and Carol K. Hall
Department of Chemical and Biomolecular Engineering, North Carolina State University, Raleigh, North Carolina 27695

ABSTRACT The pathological manifestation of nine hereditary neurodegenerative diseases is the presence within the brain of aggregates of disease-specific proteins that contain polyglutamine tracts longer than a critical length. To improve our understanding of the processes by which polyglutamine-containing proteins misfold and aggregate, we have conducted molecular dynamics simulations of the aggregation of model polyglutamine peptides. This work was accomplished by extending the PRIME model to polyglutamine. PRIME is an off-lattice, unbiased, intermediate-resolution protein model based on an amino acid representation of between three and seven united atoms, depending on the residue being modeled. The effects of hydrophobicity on the system are studied by varying the strength of the hydrophobic interaction from 12.5% to 5% of the hydrogen-bonding interaction strength. In our simulations, we observe the spontaneous formation of aggregates and annular structures that are made up of β-sheets starting from random configurations of random coils. This result was interesting because tubular protofibrils were recently found in experiments on polyglutamine aggregation and because of Perutz's prediction that polyglutamine would form water-filled nanotubes.

INTRODUCTION

The pathological manifestation of nine hereditary neurodegenerative diseases, including Huntington's disease, is the presence within the brain of aggregates of disease-specific proteins that contain polyglutamine tracts longer than a critical length (1,2). In the case of Huntington's, the associated protein is called Huntingtin. Although the causative link between the aggregation of polyglutamine-containing proteins and these so called ''polyglutamine diseases'' has not yet been firmly established, protein aggregation is widely believed to play a key role. Evidence pointing toward such a link includes the observations that the diseases occur only when the protein's polyglutamine tract is longer than a certain critical length (1,3–13) and the proteins aggregate in vitro and in vivo only when their polyglutamine tract is longer than a critical value (14–21). Furthermore, the aggregation proceeds via a nucleation and growth mechanism that speeds up as the length of the polyglutamine stretch increases (16,22–24); this may explain why the diseases manifest themselves in their victims at earlier ages as the length of the polyglutamine sequence increases.

The molecular mechanisms by which the proteins implicated in the polyglutamine diseases aggregate is still unclear. To shed light on these mechanisms and to improve our understanding of the processes by which polyglutamine-containing proteins misfold and aggregate, we have conducted molecular dynamics simulations of the aggregation of model polyglutamine peptides. Although some work has been done on simulating isolated polyglutamine molecules (25,26) and dimers of polyglutamine (27), to our knowledge these are the first molecular simulations of the aggregation of large systems of polyglutamine peptides.

Our simulations have been conducted using an intermediate-resolution protein model developed in our lab, PRIME, which is extended here to represent polyglutamine. PRIME was first introduced by Smith and Hall (28–31) and later improved by Nguyen et al. (32); it has the advantage of capturing the essential features of the forces responsible for protein folding, such as the hydrophobic effect and hydrogen bonding, yet can still be used to simulate large systems at long timescales in a reasonable time. It stands at the crossroads between the ''all-atom'' models that account for the motions of every atom on the protein being simulated, as well as every solvent atom, and the more coarse-grained models that simply represent amino acid residues or groups of amino acid residues as beads on a lattice.

Proteins containing polyglutamine tracts are thought to form β-sheets that are stabilized by hydrogen bonds not only between backbone atoms but also between atoms on glutamine side chains (33). This was first suggested by Max Perutz based on atomic-level models that showed that if polyglutamine were folded into an antiparallel β-sheet, the side-chain groups would be positioned so that an amino group on one strand could donate a hydrogen bond to a carbonyl group on the next strand (34). In this structure, the side chains lie above and below the plane of the β-sheet so that every hydrogen-bond donor on one side chain is matched with a hydrogen-bond acceptor on the next side chain (34).

Polyglutamine has been found to form β-sheets by a variety of experimental techniques including circular dichroism,

Submitted December 7, 2005, and accepted for publication February 24, 2006.

Address reprint requests to Carol K. Hall, Dept. of Chemical and Biomolecular Engineering, North Carolina State University, Engineering Bldg. I, Box 7905, 911 Partners Way, Raleigh, NC 27695-7905. Tel.: 919-515-3571; Fax: 919-515-3465; E-mail: hall@ncsu.edu.

0006-3495/06/06/4574/11 $2.00

doi: 10.1529/biophysj.105.079269

electron microscopy, and x-ray diffraction (35,36). Bevivino et al. (37) used infrared spectroscopy, circular dichroism, and electron microscopy to examine the structure of an ataxin-3 protein with an expanded polyglutamine tract and found that the polyglutamine regions adopt β-sheet structures. They also showed, using atomic-level molecular modeling, that the strands of the β-sheet need to be parallel to match every hydrogen-bond donor with a hydrogen-bond acceptor. Tanaka et al. (38) used circular dichroism, infrared spectroscopy, and electron microscopy to show that glutamine repeats adopt β-sheet structures when inserted into myoglobin. They proposed that the β-sheets are antiparallel and that when the polyglutamine sequence becomes too long, the β-sheets move to the surface of the protein, where they can more readily form intermolecular aggregates with corresponding β-sheets on other molecules. Scherzinger et al. (39) used electron microscopy to study the structure of aggregates formed from Huntington containing an expanded polyglutamine tract and found that these aggregates are fibrillar. Cooper et al. (40) stained protein fragments that contain expanded polyglutamine tracts with Congo Red dye and examined them with polarized light microscopy to show that they have β-sheet conformations. Chen et al. (24) used circular dichroism to show that synthetic polyglutamine peptides exist in β-sheet conformations.

Based on analysis of x-ray crystallographic data, Perutz et al. (41) recently suggested that polyglutamine could form β-sheets with strands that wind around to form nanotubes. The nanotube idea led naturally to the following explanation for the dependence of polyglutamine aggregation on tract length. Polyglutamine tracts of 40 residues or longer could form two turns within the nanotube structure; these would be stabilized through hydrogen bonding between the turns. This double-turn structure could then serve as a nucleus for growth of a nanotube. Polyglutamine tracts shorter than 40 residues would not be able to adopt the whole two-turn structure; structures formed by such peptides would be less stable since they would have fewer hydrogen bonds (41). This prediction is controversial and the x-ray diffraction patterns have recently been reinterpreted (42) to suggest that the peptides are in a stacked β-sheet conformation similar to the classical fibril structure (43). Recently, Sharma et al. (44) collected new x-ray diffraction data on polyglutamine aggregates and suggested that polyglutamine β-sheets stack to form slablike fibrils.

Annular structures have been observed experimentally in aggregating systems of polyglutamine and other proteins associated with diseases of the brain. Wacker et al. (45) used atomic force microscopy to examine aggregates formed from huntingtin containing a polyglutamine tract 53 residues in length and found annular structures that were themselves made up of smaller annular structures. Lashuel et al. (46) used electron microscopy to examine mutant α-synuclein proteins that are linked to Parkinson's disease and found annular structures. Ding et al. (47) used atomic force microscopy to examine α-synuclein and also found annular structures.

The β-sheets formed by polyglutamine-containing proteins assemble via a nucleated process in which the rate-limiting step is the formation of the first small section of β-sheet structure, after which the β-sheet grows quickly (16,22–24). Experimental support for this mechanism is as follows. Aggregation increases when the concentration of polyglutamine-containing proteins increases. This is consistent with a nucleation-dependent mechanism, because nucleus formation is more probable at higher concentrations (16,18). Furthermore, aggregation of polyglutamine-containing proteins is preceded by a so-called lag time, the time it takes for the nucleus to assemble. After that, aggregation proceeds rapidly as the nucleus grows (16,24,48). The lag time depends on the concentration of the aggregating protein: the higher the concentration, the more likely the nucleus is to form and the smaller the lag time (16). The lag time also depends on the length of the polyglutamine tract; longer polyglutamine peptides tend to have shorter lag times (48). Nucleation of polyglutamine aggregates can also be ''seeded'' by adding small amounts of aggregated polyglutamine (1,16,24).

Simulations have been used to study the folding of isolated polyglutamine peptides and the dimerization of small systems of two polyglutamine peptides. Starikov et al. (25) examined the structure of a 40-residue polyglutamine protein using three different all-atom simulation codes, CHARMM, AMBER, and OPLSAA. The protein folded into a β-sheet when CHARMM was used and into a compact random coil when the two other packages were used. The simulated β-sheet exhibited interstrand hydrogen bonding between donors and acceptors on the backbone but more intra- than interstrand hydrogen bonding between sites on the side chains. In the compact random coil they found many side chain-side chain hydrogen bonds. They suggested that polyglutamine chains longer than a critical chain length fold into β-hairpins, which then aggregate if the concentration is high enough for nucleation.

Finke et al. (26) developed a united-atom model for polyglutamine in which each residue is represented by two beads, one for the backbone atoms and another for the side-chain atoms. They parameterized their model so that it would agree with experiments that they conducted on CI2 proteins with polyglutamine insertions. The strengths of the various interactions in their model were adjusted so that the simulated change in stability between the CI2 protein and the CI2 protein with a polyglutamine insertion would agree with the change in stability determined experimentally. They then used their model to simulate a single CI2 protein with polyglutamine insertions and concluded that isolated short polyglutamine peptides should exist as random coils.

Stork et al. (27) used fully atomistic CHARMM simulations with explicit water molecules to measure the stability of various configurations of polyglutamine 56 and 60 residues long, as well as of two polyglutamine chains each 36 residues long. They started their simulations in two of the conformations that polyglutamine has been postulated to adopt, the nanotube and the β-helix. The nanotube configuration is the

configuration suggested by Perutz that was discussed earlier. The β-helix is similar to the nanotube except that the helix is shaped like a triangle (as opposed to being circular), with straight portions separated by three sharp turns. Stork et al. determined the stability of these configurations based on whether the peptides unfolded or remained in a particular configuration. They found that none of the tube configurations were stable, but that a β-helical peptide with three helical repeats of 18 residues and a dimer of two β-helical petides, each with two helical repeats of 18 residues, were stable.

In this article, we describe the extension of PRIME (32,49–51) (previously used to describe polyalanine) to the description of polyglutamine and present our findings on the aggregation of systems of 24 and 48 polyglutamine peptides that are 16 residues long. PRIME uses discontinuous potentials to take advantage of discontinuous molecular dynamics (DMD), a simulation technique that is very fast compared to traditional molecular dynamics calculations. Our simulations are started from random configurations of random coils at high temperatures and slowly cooled to the simulation temperature. Simulations are performed in the canonical ensemble with fixed number of particles, system volume, and temperature. The number of particles and system volume are picked to give a fixed concentration of 5 mM. The effects of hydrophobicity on the system are studied by varying the strength of the hydrophobic interaction from 12.5% to 5% of the strength of the hydrogen-bonding interaction. We monitor the aggregation of the polyglutamine peptides over a wide range of temperatures. Aggregation and aggregate structure are monitored by calculating the number of β hydrogen bonds, the percent of the peptides in β-sheets, and the number of β-regions in the system.

Highlights of our results include the following. At intermediate values of temperature we observed the spontaneous formation of β-sheets and annular structures made up of β-sheets. These annular structures resemble nanotubes and β-barrels. The number of peptides in β-sheets decreases with increasing temperature. At the very highest temperatures, the system does not fold or aggregate; it remains a system of isolated random coils. At low temperatures, amorphous aggregates are formed.

The organization of this article is as follows. In Methods, the peptide model and the simulation method are described. In Results, we present our results on the formation of β-sheets, the formation of annular structures made up of β-sheets, and the effects of hydrophobicity on the aggregation of our model polyglutamine peptides. The last section contains a discussion of our results.

METHODS

Model forces

In this work, we extend the protein model PRIME (PRotein Intermediate resolution ModEl) to polyglutamine. PRIME was originally developed by Smith and Hall (28–31), inspired by the work of Takada et al. (52), and improved upon by Nguyen et al. (32). This model is designed to be used with a simulation technique known as discontinuous molecular dynamics (DMD) (53–55), an extremely fast alternative to traditional molecular dynamics. DMD simulations are appropriate for systems with discontinuous potentials such as hard-sphere and square-well potentials, where the forces operating on the molecules change only at specific points in time and space when the particles collide. In contrast, the forces in traditional molecular dynamics simulations (which are based on continuous potentials) change at all points in space and time. DMD simulations are much faster than traditional molecular dynamics simulations because Newton's laws can be solved analytically instead of by numerically integrating the potentials. Furthermore, the time course of the simulation is not restricted to small, equally spaced time steps as is the case with traditional molecular dynamics; instead, the entire system can advance in time to the next discontinuity in the potential, which is referred to as an ''event.''

PRIME is an off-lattice, unbiased, intermediate-resolution protein model (28–32) that has thus far been applied mainly to polyalanine. Each amino acid residue is composed of a three-sphere backbone comprised of united atoms NH, $C_\alpha H$, and C=O. An alanine side chain is represented by one sphere. PRIME has realistic bond lengths and bond-angle constraints and has the ability to interact both intra- and intermolecularly via hydrogen bonding and hydrophobic interaction potentials. All backbone bond lengths and bond angles are fixed at their ideal values; the distance between consecutive C_α atoms is fixed so as to maintain the interpeptide bond in the *trans* configuration. The side chains are held in positions relative to the backbone so that all residues are L-isomers. The effect of solvent is factored into the energy function as a potential of mean force.

All forces are modeled by discontinuous potentials. The excluded volumes of the united atoms are modeled using hard-sphere potentials with realistic diameters. Covalent bonds are maintained between adjacent spheres along the backbone by imposing hard-sphere repulsions whenever the bond lengths attempt to move outside of the range between $(1 - \delta)\ell$ and $(1 + \delta)\ell$, where ℓ is the bond length and δ is a tolerance that we set to 2.5%. Ideal backbone bond angles, C_α-C_α distances, and residue L-isomerization are achieved by imposing pseudobonds, which also fluctuate within a tolerance of 2.5%. Interactions between hydrophobic side chains are represented by a square-well potential of depth ϵ_{HP} and range $1.5\sigma_R$ where σ_R is the side-chain united-atom diameter. Hydrophobic side chains must be separated by at least one intervening residue to interact. Hydrogen bonding between amide hydrogen atoms and carbonyl oxygen atoms on the same or neighboring chains is represented by a square-well potential of depth ϵ_{HB} between NH and C=O united atoms whenever 1), the virtual hydrogen and oxygen atoms (whose location can be calculated at any time) are separated by 4.2 Å (the sum of the NH and C=O well widths); 2), the nitrogen-hydrogen and carbon-oxygen vectors point toward each other within a fairly generous tolerance; 3), neither the NH nor the C=O are already involved in a hydrogen bond with a different partner; and 4), the NH and C=O are separated by at least one intervening residue along the chain. We allow hydrogen bonds between groups separated by one intervening residue along the chain because this reproduces the distributions of separations along the chain of hydrogen-bonding pairs observed in structures from the Protein Data Bank by Stickle et al. (56). To satisfy the requirement that the nitrogen-hydrogen and carbon-oxygen vectors point toward each other, we used the approach of Nguyen et al. (32) but the parameter set of Ding et al. (57). This parameter set allows formation of hydrogen bonds at all temperatures while still reproducing the hydrogen-bond angle and distance distributions of Smith and Hall (29). The reason we did not use the parameter set of Nguyen et al. (32) is that β-sheets formed in simulations with that parameter set at temperatures just below the β-sheet/random coil transition temperature were unphysical in that they had very few hydrogen bonds. This happened in our polyglutamine simulations but not in the polyalanine simulations of Nguyen and Hall (49–51), because the additional hydrophobic bead on the polyglutamine side chains held the polyglutamine β-strands together in a β-sheet-like structure at higher temperatures and this parameter set makes it harder for hydrogen bonds to form at high temperatures. Since β-sheets with

few hydrogen bonds are physically unrealistic, we used the parameter set of Ding et al. (57). We define the reduced temperature, T^* as kT/ϵ_{HB} and the relative hydrophobicity, R, as $\epsilon_{HP}/\epsilon_{HB}$.

PRIME is extended to polyglutamine by adopting a more complex side chain representation. We considered a variety of approaches, including a two-sphere representation, but eventually settled on a four-sphere side-chain representation since this gives the most faithful representation of the geometry of glutamine side chains. The four-sphere representation allows us to model the polyglutamine side chain with the same level of detail as the PRIME model backbone. Each side chain is represented by four spheres, as depicted in Fig. 1. Spheres 1 and 2 (as labeled in Fig. 1) each represent a methylene group and have hard cores that are surrounded by square wells to mimic excluded volume and hydrophobic interactions. Sphere 3 represents a carbonyl group; it has a hard core to mimic excluded volume and a directionally dependent square well to mimic a hydrogen-bond acceptor. Sphere 4 represents an amine group; it has a hard core to mimic excluded volume and a directionally dependent square well to mimic a hydrogen-bond donor. The four spheres all have their bond angles constrained by a system of pseudobonds. The methyl, carbonyl, and amine groups on the polyglutamine side chain are modeled in the same way as the methyl, carbonyl, and amine groups in the polyalanine PRIME model and, as such, have exactly the same sizes, bond lengths, pseudobond lengths, interaction strengths, and interaction ranges.

Discontinuous molecular dynamics

DMD simulations are conducted as follows. Each sphere of the model protein chain is assigned a random initial position that does not violate any of the size constraints or assigned bond lengths and angles. It is also assigned an initial velocity chosen at random from a Maxwell-Boltzmann distribution at a specified reduced temperature, T^*. The simulation proceeds according to the following schedule: identify the first event, move forward in time until that event occurs, calculate new velocities for the pair of spheres involved in the event and calculate any changes in system energy resulting from hydrogen bond events or hydrophobic interactions, find the second event, and so on. Types of events include excluded-volume events, covalent-bond events, pseudobond events, square-well hydrogen-bond events, and square-well hydrophobic-interaction events. An excluded-volume event occurs when the surfaces of two hard spheres collide and repel each other. A bond (or pseudobond) event occurs when two adjacent spheres attempt to move outside of their assigned bond length and the two particles feel an infinite repulsion that forces them back into their assigned bond length. Square-well events include well-capture, well-bounce, and well-dissociation ''collisions'' when a sphere enters, attempts to leave, or leaves the square well of another sphere. For more details on DMD simulations with square-well potentials, see articles by Alder and Wainwright (53) and Smith et al. (58).

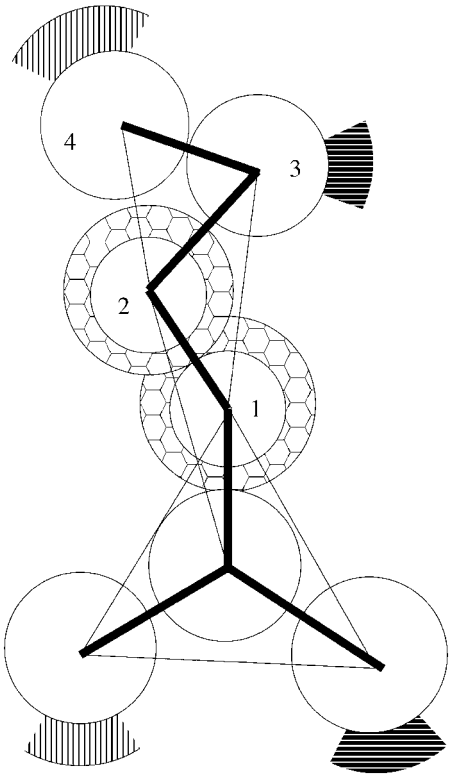

FIGURE 1 Four-sphere representation of a polyglutamine side chain. Hard spheres are white. Square wells representing hydrophobic interactions are shown in a honeycomb pattern. Square wells representing hydrogen-bond acceptors have thick horizontal stripes and square wells representing hydrogen-bond donors have thin vertical stripes. Covalent bonds are shown in bold and pseudobonds to constrain bond angles are thin lines.

The simulations were performed in the canonical ensemble, which means that the number of particles, volume, and temperature are held constant. The number of particles and box volume were picked to give the desired concentration. Between three and five simulations were run at every data point. Simulations of 24 chains were run for 30 billion DMD events and simulations of 48 chains were run for 80 billion DMD events, to ensure that a stable structure was formed. Properties were averaged over the last 2 billion DMD events, and error bars represent the standard deviation between all the runs at a given state point. Periodic boundary conditions were used to eliminate artifacts due to simulation box walls. The Andersen thermostat (59) was used to maintain constant temperature; in this method, all the particles experience random, infrequent events where they are given a new velocity selected randomly from a Maxwell-Boltzmann distribution centered at the simulation temperature. These events are referred to as ''ghost collisions'' or collisions with ''ghost particles.''

Systems containing 24 and 48 chains at a concentration of 5 mM were slowly quenched from a random configuration of high-temperature random coils at $T^* = 0.5$ to the temperature of interest, which ranged from $T^* = 0.075$ to $T^* = 0.205$. Simulations at relative hydrophobicity $R = 0.05, 0.075, 0.1$, and 0.125 were performed to learn how the strength of this interaction affects the self-assembly of the peptides in the system. We monitored the number of β backbone-backbone hydrogen bonds, which we define as hydrogen bonds in which both the donor and acceptor backbone dihedral angles, ϕ and ψ, adjacent to the hydrogen bond lie in the range $0 \le \psi \le 180$ and $-180 \le \phi \le -30$. This range for the dihedral angles is the same as that used by Nguyen et al. (32). We also monitored the number of backbone-backbone, side chain-side chain, and side chain-backbone hydrogen bonds, as well as the fraction of peptides in β-sheets and the number of β-regions (defined below). The fraction of peptides in β-sheets was calculated based on the following definitions. A β-sheet is defined as a structure in which two or more peptides share a number of β hydrogen bonds between them that is greater than or equal to half the chain length (eight hydrogen bonds in the case of our 16-residue chains). This definition emerged from the observation that if two peptides are perfectly aligned, the number of hydrogen bonds between them could equal the chain length. Although the N and C spheres associated with each residue could both form hydrogen bonds, the direction in which the residues face alternates along the chain from facing the peptide in question to facing away from the peptide in question. Thus, the maximum possible number of hydrogen bonds between them would equal the chain length. The fraction of peptides in β-sheets is the number of peptides involved in β-sheet structures divided by the total number of peptides in the system. We were also interested in the contiguousness of the β hydrogen bonds, so we defined a β-region to be a section in an aggregate where two neighboring peptides share at least five β hydrogen bonds in a row. Since the residues alternate between facing toward and away from each other, the term ''in a row'' does not include the two hydrogen bonds formed when the residues in question face away from each other. Thus, five in a row means hydrogen bonds formed by N_i, C_i, N_{i+2}, C_{i+2}, N_{i+4}, or C_i, N_{i+2}, C_{i+2}, N_{i+4}, C_{i+4}, where i is the residue number along the chain.

RESULTS

DMD simulations were performed on systems containing 24 and 48 16-residue polyglutamine chains to see if they would form fibrils. We chose a chain length of 16 because Nguyen and Hall (49) found that systems containing polyalanine chains 16 residues long that were initially in random coil conformations spontaneously formed fibrils as the simulations progressed. We found that as our simulations progressed the polyglutamine peptides folded into β-sheets that tended to curve. When there were enough peptides in the system, the β-sheets rolled up into a tubelike structure that resembled a classic β-barrel. Snapshots of one of the resulting tube structures are shown in Fig. 2. The tube in this figure contains 11 peptides and has an inner diameter of 17–18 Å, an outer diameter of 41–43 Å, and a height of 30–45 Å.

We observed a variety of tube morphologies in our simulations, including tubes with large diameters (Fig. 3 *A*), tubes that are connected to each other (Fig. 3 *B*), and tubes connected to β-sheets (Fig. 3 *C*). The large tube shown in Fig. 3 *A* has an inner diameter of 32–39 Å, an outer diameter of 55–62 Å, and a height of 43–49 Å.

We examined the self-assembly of these structures at relative hydrophobicity values of R = 0.005, 0.075, 0.10, and 0.125 to find a reasonable value for this parameter, which is the only adjustable parameter in the model. It is difficult to assign a value to this parameter a priori, because we are coarse-graining away detail not only about the hydrogen-bond donors and acceptors but also about the solvent molecules. Since little is known about the molecular-level structure of polyglutamine aggregates, besides that they are made up of β-sheets (at this point a controversy exists as to whether these β-sheets form ringlike structures (41,45) or slablike fibrils (42,44)), it would be useful to know the value of the relative hydrophobicity at which the system self-assembles into the most ordered β-sheets. This value could then be used in future simulations.

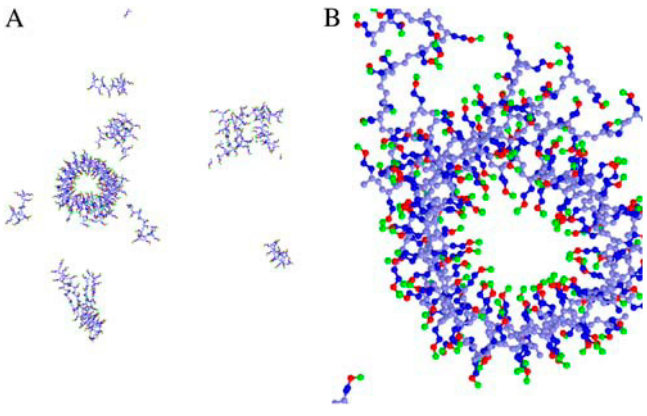

FIGURE 2 (*A*) Snapshot of the whole system of 24 polyglutamine 16-mers at $R = 0.125$, $T^* = 0.155$. (*B*) Close-up of the tube formed from 24 polyglutamine 16-mers at $R = 0.125$, $T^* = 0.155$.

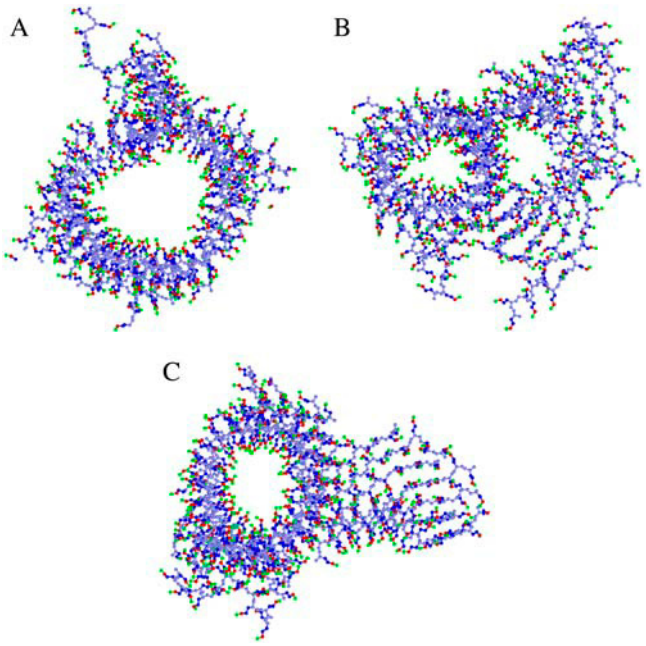

FIGURE 3 (*A*) Snapshot of large diameter tube formed by 24 polyglutamine 16-mers at $R = 0.125$, $T^* = 0.185$. (*B*) Snapshot of connected tubes morphology formed by 24 polyglutamine 16-mers at $R = 0.125$, $T^* = 0.185$. (*C*) Snapshot of tube connected to sheet morphology formed from 24 polyglutamine 16 mers at $R = 0.125$, $T^* = 0.165$.

Fig. 4 shows the number of β intermolecular backbone-backbone hydrogen bonds as a function of T^* at the four different values of the relative hydrophobicity. At all R, the system shows the following behavior as a function of the reduced temperature. At low T^*, the system has a small number of β intermolecular hydrogen bonds, because it is in a collapsed state that is relatively disordered. As T^* increases, the system forms more and more β intermolecular hydrogen bonds because it has more flexibility, which gives it the freedom to find more ordered states. At high T^*, the number of β intermolecular hydrogen bonds decreases as temperature increases because entropy takes over and the peptides become increasingly random-coil-like.

The value of the relative hydrophobicity, R, affects the self-assembly of the peptides as follows. At the highest values of the relative hydrophobicity ($R = 0.125$), the system remains in a β-sheet conformation for higher values of T^* than it does at all the other values of the relative hydrophobicity. It also has fewer β intermolecular hydrogen bonds at low temperatures than systems at intermediate values of the hydrophobicity ($R = 0.1$ and $R = 0.075$). As the hydrophobic interaction decreases from $R = 0.125$ to $R = 0.05$, the T^* at which the system transitions from β-sheets to random coils decreases. Additionally, as the hydrophobic interaction decreases from $R = 0.1$ to $R = 0.05$, the low value of T^* at which the peptides undergo a transition from β-sheets to amorphous aggregates increases. Thus, the range of T^* over which the system self-assembles into β-sheets becomes narrower as the

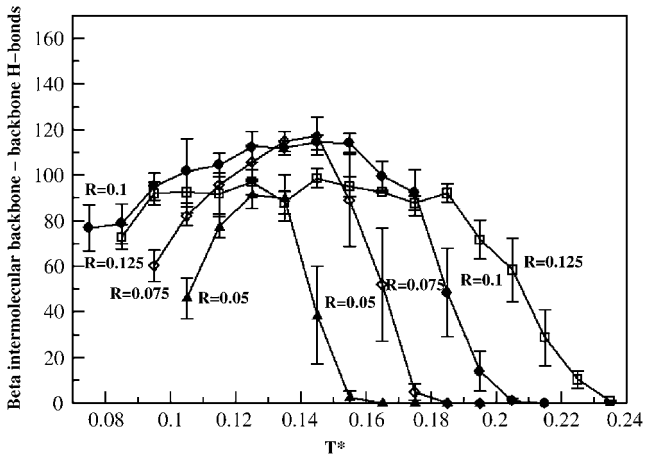

FIGURE 4 β-intermolecular backbone-backbone hydrogen bonds versus T^* for the 24 polyglutamine 16-mers system.

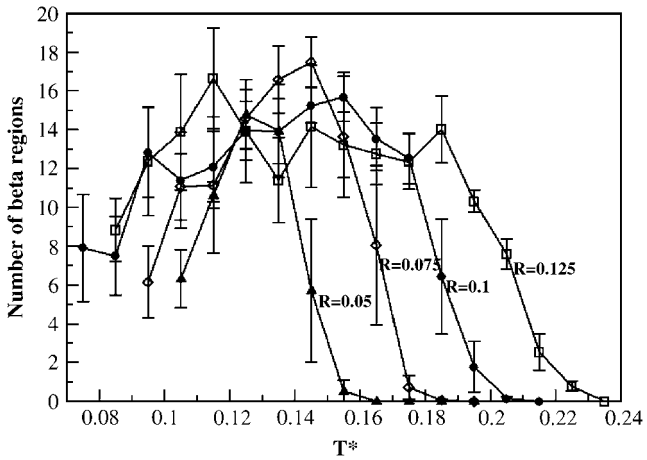

FIGURE 6 Number of β-regions versus T^* for the 24 polyglutamine 16-mers system.

hydrophobic interaction strength decreases. At low values of the hydrophobic interaction ($R = 0.05$), the peptides do not self-assemble into β-sheets as well as they do at higher values of R, because they do not have as many β intermolecular backbone-backbone hydrogen bonds as the systems at higher values of R. At high values of the hydrophobic interaction ($R = 0.125$) the peptides do not self-assemble into β-sheets as well as they do at lower values of R, because they get caught in kinetic traps more easily due to the strength of the hydrophobic attraction.

To quantify the structure of the aggregates that are formed, we have determined the fraction of peptides that are in β-sheets and the number of β-regions in the system. Fig. 5 shows the fraction of peptides that are in β-sheets versus T^* for all the hydrophobic interaction strengths studied. Fig. 6 shows the number of β-regions versus T^* for all the hydrophobic interaction strengths studied.

The trends seen in Fig. 4 are also seen in Figs. 5 and 6. At low values of T^*, the system is kinetically trapped in amorphous structures and hence all measures of β-sheet formation are low. As T^* increases, all of the curves go through a maximum at an optimum temperature for β-sheet formation. As T^* increases further, the system undergoes a transition to random coils because entropy is taking over. As the hydrophobicity increases, the temperature at which the transition from β-sheets to random coils occurs increases and the temperature at which the transition from β-sheets to amorphous aggregates occurs decreases. This trend is not followed, however, at the highest value of the relative hydrophobicity, $R = 0.125$. In this case, the fraction of peptides in β-sheets is generally lower than at the other values of the relative hydrophobicity. This happens because the system gets caught in kinetic traps more easily due to the very strong hydrophobic interaction.

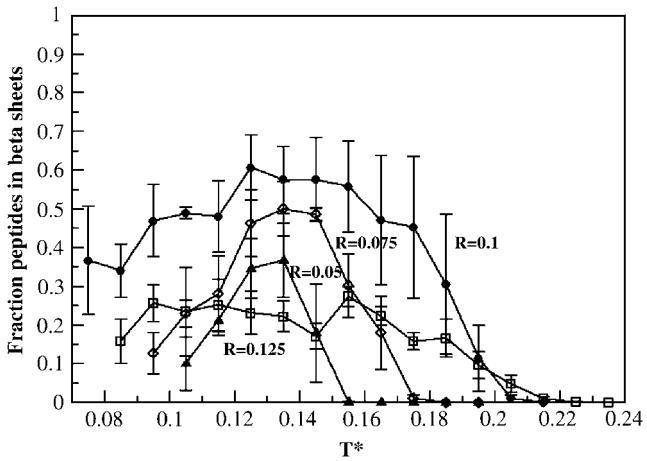

FIGURE 5 Fraction peptides in β-sheets versus T^* for the 24 polyglutamine 16-mers system.

At intermediate values of the relative hydrophobicity, $R = 0.1$ and $R = 0.075$, the peptides assemble into β-sheets at intermediate values of reduced temperature $T^* = 0.115$ to $T^* = 0.155$ almost equally well. The system at relative hydrophobicity $R = 0.075$ has slightly more β intermolecular backbone-backbone interactions and β-regions than the system at the hydrophobicity $R = 0.1$ at reduced temperatures of $T^* = 0.135$ and $T^* = 0.145$ but a lower fraction of peptides in β-sheets. Based on these observations we believe that the lower of these two relative hydrophobicities, $R = 0.075$, allows the system to make β-sheets that are more ordered (based on having more β-regions) but smaller (based on the fraction of peptides in β-sheets). Evidently, the hydrophobicity at $R = 0.1$ is strong enough that it prevents the peptides from optimally arranging into very well ordered β-sheets and the hydrophobicity at $R = 0.075$ is weak enough that the entire system does not aggregate into β-sheets.

To check to see if these trends would be followed for larger systems, we performed simulations on larger systems containing 48 polyglutamine 16-mers at $R = 0.075$ and $R = 0.10$. We found similar behavior for the β intermolecular

backbone-backbone hydrogen bonds and β-regions. However, the fraction of peptides in β-sheets was different in that the maximum at $R = 0.075$ was higher than the maximum at $R = 0.10$ (the opposite was the case for the smaller system). This result can be seen in Fig. 7. We believe that this is because the larger systems are more prone to getting caught in kinetic traps at high hydrophobicity. We conclude that the relative hydrophobicity value $R = 0.075$ is most appropriate for future simulations with this model.

The peptides at the lowest value of the hydrophobicity, $R = 0.05$, are least likely to self-assemble into β-sheets. Our explanation for this is that hydrophobicity, a side chain-side chain interaction, which brings the side chains together (when strong enough), promotes the formation of side chain-side chain hydrogen bonds. Once the side-chain united atoms have formed hydrogen bonds with other side-chain united atoms they are unlikely to break and form hydrogen bonds with backbone united atoms. This then permits the backbone united atoms to form hydrogen bonds with other backbone united atoms without interference from side-chain united atoms. However, if the hydrophobicity is low, the side-chain united atoms will be less likely to hydrogen-bond with other side-chain united atoms, opening the door to hydrogen bonding between side chain united atoms and backbone united atoms. These side chain-backbone hydrogen bonds interfere with the formation of backbone-backbone hydrogen bonds, leading to the formation of more amorphous structures.

This increased side chain-backbone hydrogen bonding at low values of the relative hydrophobicity ($R = 0.05$) can be seen by comparing the numbers of total backbone-backbone, β backbone-backbone, side chain-side chain, and side chain-backbone intermolecular hydrogen bonds plotted in Figs. 8 and 9 as a function of T^* at $R = 0.075$ and $R = 0.05$, respectively. At both values of hydrophobicity, as the reduced temperature decreases, the number of side chain-backbone hydrogen bonds formed increases. The total

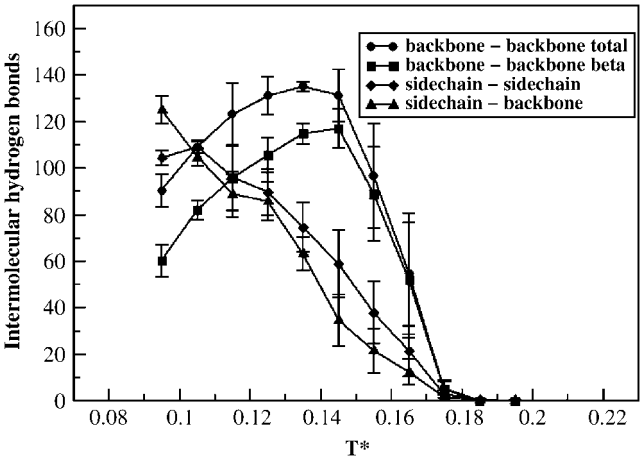

FIGURE 8 Intermolecular hydrogen bonds versus T^* at $R = 0.075$ for the 24 polyglutamine 16-mers system.

number of backbone-backbone hydrogen bonds and the number of β backbone-backbone hydrogen bonds decrease after going through a maximum at intermediate values of T^*. The system at the hydrophobicity of $R = 0.075$ is more likely to form β-sheets at intermediate values of T^* (as indicated by the large numbers of β intermolecular backbone-backbone hydrogen bonds at these T^* values) than the system at the hydrophobicity of $R = 0.05$. This is because for $R = 0.05$, when T^* is low enough to bring all the peptides in the system together, too many side chain-backbone hydrogen bonds form and at higher values of T^*, the system forms small β-sheets and random coils. At this low value of the relative hydrophobicity, the peptides go from amorphous aggregates dominated by side chain-backbone interactions at low values of T^* (as indicated by the large numbers of intermolecular side chain-backbone hydrogen bonds at these T^* values) to the transition from one large aggregate to smaller and smaller β-sheets and eventually random coils at higher T^* values

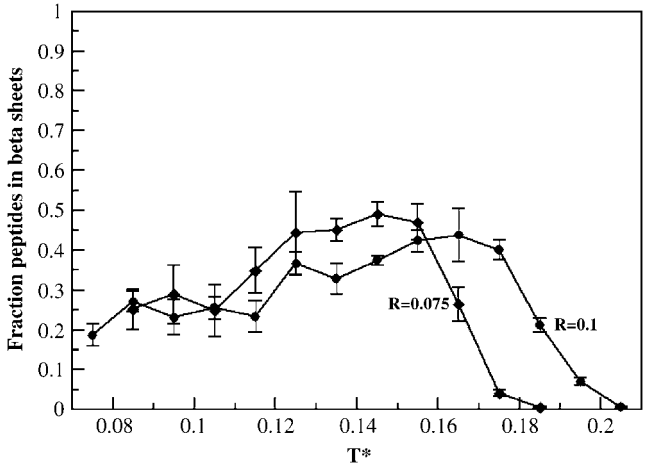

FIGURE 7 Fraction peptides in β-sheets versus T^* for the 48 polyglutamine 16-mers system.

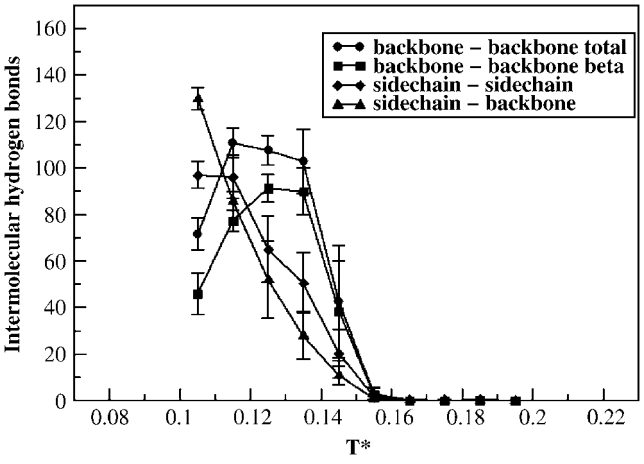

FIGURE 9 Intermolecular hydrogen bonds versus T^* at $R = 0.05$ for the 24 polyglutamine 16-mers system.

(as indicated by the decrease in intermolecular backbone-backbone hydrogen bonds as T^* increases).

To determine the role played by the side chain-backbone hydrogen bonding in the increased amorphous aggregation at low values of relative hydrophobicity and temperature and in the formation of annular structures, we performed simulations with this interaction turned off. Side chain-side chain and backbone-backbone hydrogen bonds were allowed, but side chain-backbone hydrogen bonds were not. As can be seen in Fig. 10, by comparing the filled-circle and asterisk curves, removing the possibility of side chain-backbone hydrogen bonding increased the number of β intermolecular backbone-backbone hydrogen bonds, which means that the structures were more ordered and therefore less amorphous. Annular structures were also observed in these simulations. We concluded that the side chain-backbone hydrogen bonds were causing increased amorphous aggregation, and that annular structures could be formed without these interactions.

We were also interested in the effects of the side chain-side chain hydrogen bonding on the aggregation of our model polyglutamine peptides so we performed simulations with all of the side-chain hydrogen bonding turned off. In this case, backbone-backbone hydrogen bonds were the only hydrogen bonds allowed to form. As can be seen in Fig. 10, there was an increase in the number of β intermolecular backbone-backbone hydrogen bonds (*curve with open circles*) compared to the number in the simulations with side chain-backbone and side chain-side chain hydrogen bonds allowed (*curve with solid circles*) and an increase compared to the simulations performed with side chain-side chain hydrogen bonds allowed but side chain-backbone hydrogen bonds turned off (*curve with asterisks*). Annular structures were also observed in these simulations. We concluded that the side chain-side chain hydrogen bonding

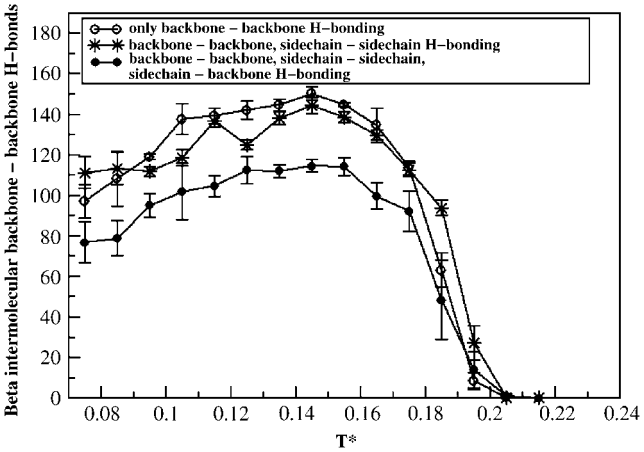

FIGURE 10 β-Intermolecular backbone-backbone hydrogen bonds versus T^* for the polyglutamine 16-mers system at $R = 0.1$ with all side-chain hydrogen bonding turned on (*solid circles*), side chain-backbone hydrogen bonding turned off (*asterisks*), and all side-chain hydrogen bonding turned off (*open circles*).

was increasing the complexity of the energy landscape for the system and therefore increasing kinetic trapping which led to less ordered structures. Furthermore we concluded that the side chain hydrophobicity and backbone-backbone hydrogen bonding were sufficient for the formation of annular structures by polyglutamine.

In developing the models used for polyglutamine, we performed simulations of isolated polyglutamine peptides 16 residues long with the side-chain hydrogen-bonding interactions both turned off and turned on. We found that when the side chain hydrogen-bonding interactions were turned on, the peptides folded into structures we call ''collapsed random coils'', since they had few α or β backbone-backbone hydrogen bonds. However, when the side-chain hydrogen-bonding interactions were turned off, these peptides folded into α-helices. Since evidence to date suggests that polyglutamine does not fold to a unique conformation, but instead adopts a random-coil conformation (24,60), we believe that the polyglutamine model without side-chain hydrogen bonding is not a good one, as the peptides will fold into α-helices in this case.

In a set of simulations on a small system of eight polyglutamine chains 16 residues long with all of the side-chain hydrogen bonding turned off and the hydrophobicity of the γ-side chain methyl group (the second sphere from the backbone on the side chain) turned off, we noticed that the peptides did not aggregate. Instead, there was a transition from α-helices directly to random coils as temperature was increased. This means that both methyl groups on the side chain need to have the hydrophobic interactions for the model polyglutamine peptides to form β-sheets and annular structures.

We believe that the lack of an attraction between the side-chain end groups (the amine spheres) is what is leading to the formation of annular structures by our model polyglutamine molecules as opposed to the slablike fibril structures that were formed in the simulations of Nguyen and Hall (49–51). In the simulations with all of the side-chain hydrogen bonding turned off, the carbonyl and amine spheres behaved as hard spheres. Essentially, because there was no attraction between these side chain end groups there was no force driving the β-sheets to stack. Instead they formed one large β-sheet, which then rolled into an annular structure to avoid having exposed β-sheet ends (which are energetically unfavorable because of unsatisfied hydrogen bonds). To test this idea, we are currently developing a model in which the carbonyl and amine spheres interact via a square-well attraction to mimic van der Waals forces to see what effects this will have on the structures formed as the peptides aggregate.

DISCUSSION

Our short polyglutamine chains formed β-sheets that curved to make nanotubes. This result was interesting because tubular protofibrils were recently found in experiments on

polyglutamine aggregation (45) and in experiments on the protein responsible for Parkinson's disease, α-synuclein (46,47), and because of the growing interest in using proteins in nanoscience (61–73). Our results are also intriguing given the prediction of Perutz et al. that polyglutamine should form water-filled nanotubes (41). Although this prediction was made for polyglutamine peptides 40 residues long and suggested a tube diameter of 11.8 Å, our finding that our model polyglutamine peptides 16 residues long formed tubes with diameters of 17 Å is still interesting. Perutz et al. based their prediction on x-ray scattering of aggregates of peptides containing 15 glutamine residues, so our findings in simulations of aggregation of polyglutamine peptides 16 residues long are more comparable with their experimental results than with their predictions of structures for polyglutamine peptides 40 residues long. We wish to point out that this prediction is controversial and that their x-ray diffraction patterns have recently been reinterpreted (42) to suggest that the peptides are in a stacked β-sheet conformation similar to the classical fibril structure (43). Likewise, recent x-ray diffraction work by Sharma et al. (44) has suggested that polyglutamine forms slablike fibrils. Since this controversy exists as to how polyglutamine β-sheets are organized in aggregates, we are unable to conclusively verify our predicted molecular structures for polyglutamine aggregates against experimentally determined molecular structures. Hopefully this situation will change in the near future, as research workers begin to apply the powerful solid-state NMR technique to polyglutamine-containing proteins.

It is important to point out the limitations of our model and our methodology that arise because of compromises we have made to be able to study protein aggregation within the limit of today's computational technology. The absence of explicit water molecules in our simulations is a limitation, because it does not allow us to account for hydrogen bonding between backbone atoms and water molecules or between side-chain atoms and water molecules. Furthermore, as Perutz et al. predicted, the polyglutamine nanotube should be filled with water, which means that water molecules could potentially play an important role in these structures. The lack of atomistic detail does not allow us to accurately account for the packing of all the atoms or predict the energetics of the system with any accuracy. Finally our potential of mean force for the hydrophobic effect does not change with temperature. Nonetheless, the compromises that we have made in model detail are necessary to be able to treat the large system sizes and long timescales characteristic of aggregation phenomena.

We are currently performing simulations of longer chains closer to the critical repeat length for Huntington's disease to contribute more directly to Huntington's disease research. These results will be presented in a forthcoming article.

We thank Dr. Andrew J. Schultz for his help in speeding up our discontinuous molecular dynamics simulations. We thank the North Carolina State University High-Performance Computing Center for computer time.

This work was supported by a National Institutes of Health Molecular Biology Training Program fellowship and by National Institutes of Health grant GM-56766.

REFERENCES

1. Wanker, E. E. 2000. Protein aggregation and pathogenesis of Huntington's disease: mechanisms and correlations. *Biol. Chem.* 381:937–942.
2. Bates, G. 2003. Huntingtin aggregation and toxicity in Huntington's disease. *Lancet.* 361:1642–1644.
3. MacDonald, M. E., C. M. Ambrose, M. P. Duyao, R. H. Myers, C. Lin, L. Srinidi, G. Barnes, S. A. Taylor, M. James, N. Groot, H. McFarlane, B. Jenkins, et al. 1993. A novel gene containing a trinucleotide repeat that is expanded and unstable on Huntington's disease chromosomes. *Cell.* 72:971–983.
4. Orr, H. T., M. Chung, S. Banfi, T. J. K. Jr, A. Servadio, A. L. Beaudet, A. E. McCall, L. A. Duvick, L. P. W. Ranum, and H. Y. Zoghbi. 1993. Expansion of an unstable trinucleotide CAG repeat in spinocerebellar ataxia type 1. *Nat. Genet.* 4:221–226.
5. Banfi, S., A. Servadio, M. Chung, T. J. Kwiatkowski, Jr., A. E. McCall, L. A. Duvick, Y. Shen, E. J. Roth, H. T. Orr, and H. Y. Zoghbi. 1994. Identification and characterization of the gene causing type 1 spinocerebellar ataxia. *Nat. Genet.* 7:513–520.
6. Kawaguchi, Y., T. Okamoto, M. Taniwaki, M. Aizawa, M. Inoue, S. Katayama, H. Kawakami, S. Nakamura, M. Nishimura, I. Akiguchi, J. Kimura, S. Narumiya, and A. Kakizuka. 1994. CAG expansions in a novel gene for Machado-Joseph disease at chromosome 14q32.1. *Nat. Genet.* 8:221–228.
7. Nagafuchi, S., H. Yanagisawa, K. Sato, T. Shirayama, E. Ohsaki, M. Bundo, T. Takeda, K. Tadokoro, I. Kondo, N. Maurayama, Y. Tanaka, H. Kikushima, et al. 1994. Dentatorubral and pallidoluysian atrophy expansion of an unstable CAG trinucleotide on chromosome 12p. *Nat. Genet.* 6:14–18.
8. Koide, R., T. Ikeuchi, O. Onodera, H. Tanaka, S. Igarashi, K. Endo, H. Takahashi, R. Kondo, A. Ishikawa, T. Hayashi, M. Saito, A. Tomoda, et al. 1994. Unstable expansion of CAG repeat in hereditary dentatorubral-pallidoluysian atrophy (DRPLA). *Nat. Genet.* 6:9–13.
9. Housman, D. 1995. Gain of glutamines, gain of function? *Nat. Genet.* 10:3–4.
10. Trottier, Y., Y. Lutz, G. Sevanin, G. Cancel, F. Saudou, C. Weber, G. David, L. Tora, Y. Agid, A. Brice, and J. Mandel. 1995. Polyglutamine expansion as a pathological epitope in Huntington's disease and four dominant cerebellar ataxias. *Nature.* 378:403–406.
11. Sanpei, K., H. Takano, S. Igarashi, T. Sato, M. Oyake, H. Saski, A. Wakisaka, K. Tashiro, Y. Ishida, T. Ikeuchi, R. Koide, M. Saito, et al. 1996. Identification of the spinocerebellar ataxia type 2 gene using a direct identification of repeat expansion and cloning technique, DIRECT. *Nat. Genet.* 14:277–284.
12. Imbert, G., F. Saudou, G. Yvert, D. Devys, Y. Trottier, J. Garnier, C. Weber, J. Mandel, G. Cancel, N. Abbas, A. Durr, O. Didierjean, et al. 1996. Cloning of the gene for spinocerebellar ataxia 2 reveals a locus with high sensitivity to expanded CAG/glutamine repeats. *Nat. Genet.* 14:285–291.
13. Zhuchenko, O., J. Bailey, P. Bonnen, T. Ashizawa, D. W. Stockton, C. Amos, W. B. Dobyns, S. H. Subramony, H. Y. Zoghbi, and C. C. Lee. 1997. Autosomal dominant cerebellar ataxia (SCA6) associated with small polyglutamine expansions in the α 1A-voltage-dependent calcium channel. *Nat. Genet.* 15:62–69.
14. Martindale, D., A. Hackam, A. Wieczorek, L. Ellerby, C. Wellington, K. McCutcheon, R. Singaraja, P. Kazemi-Esfarjani, R. Devon, S. U. Kim, D. E. Bredesen, F. Tufaro, and M. R. Hayden. 1998. Length of huntingtin and its polyglutamine tract influences localization and frequency of intracellular aggregates. *Nat. Genet.* 18:150–154.
15. Li, S.-H., and X.-J. Li. 1998. Aggregation of N-terminal huntingtin is dependent on the length of its glutamine repeats. *Hum. Mol. Genet.* 7:777–782.

16. Scherzinger, E., A. Sittler, K. Schweiger, V. Heisner, R. Lurz, R. Hasenbank, G. P. Bates, H. Lehrach, and E. E. Wanker. 1999. Self-assembly of polyglutamine-containing huntingtin fragments into amyloid-like fibrils: implications for Huntington's disease pathology. *Proc. Natl. Acad. Sci. USA.* 96:4604–4609.

17. Lunkes, A., Y. Trottier, J. Fagart, P. Schultz, G. Zeder-Lutz, D. Moras, and J. Mandel. 1999. Properties of polyglutamine expansion in vitro and in a cellular model for Huntington's disease. *Philos. Trans. R. Soc. Lond. B Biol. Sci.* 354:1013–1019.

18. de Cristofaro, T., A. Affaitati, L. Cariello, E. V. Avvedimento, and S. Varrone. 1999. The length of polyglutamine tract, its level of expression, the rate of degradation, and the transglutaminase activity influence the formation of intracellular aggregates. *Biochem. Biophys. Res. Commun.* 260:150–158.

19. Kazantsev, A., E. Preisinger, A. Dranovsky, D. Goldgaber, and D. Housman. 1999. Insoluble detergent-resistant aggregates form between pathological and nonpathological lengths of polyglutamine in mammalian cells. *Proc. Natl. Acad. Sci. USA.* 96:11404–11409.

20. Hollenbach, B., E. Scherzinger, K. Schweiger, R. Lurz, H. Lehrach, and E. E. Wanker. 1999. Aggregation of truncated GST-HD exon 1 fusion proteins containing normal range and expanded glutamine repeats. *Philos. Trans. R. Soc. Lond. B Biol. Sci.* 354:991–994.

21. Chen, S., and R. Wetzl. 2001. Solubilization and disaggregation of polyglutamine peptides. *Protein Sci.* 10:887–891.

22. Kobayashi, D. E. M. Y., C. K. Bailey, A. A. Taye, and K. H. Fischbeck. 1998. Cleavage, aggregation and toxicity of the expanded androgen receptor in spinal and bulbar muscular atrophy. *Hum. Mol. Genet.* 7:693–701.

23. Heiser, V., E. Scherzinger, A. Boeddrich, E. Nordhoff, R. Lurz, N. Schugardt, H. Lehrach, and E. E. Wanker. 2000. Inhibition of huntingtin fibrillogenesis by specific antibodies and small molecules: implications for Huntington's disease therapy. *Proc. Natl. Acad. Sci. USA.* 97:6739–6744.

24. Chen, S., V. Berthelier, J. B. Hamilton, B. O'Nuallain, and R. Wetzel. 2002. Amyloid-like features of polyglutamine aggregates and their assembly kinetics. *Biochemistry.* 41:7391–7399.

25. Starikov, E. B., H. Lerach, and E. E. Wanker. 1999. Folding of oligoglutamines: a theoretical approach based upon thermodynamics and molecular mechanics. *J. Biomol. Struct. Dyn.* 17:409–427.

26. Finke, J. M., M. S. Cheung, and J. N. Onuchic. 2004. A structural model of polyglutamine determined from a host-guest method combining experiments and landscape theory. *Biophys. J.* 87:1900–1918.

27. Stork, M., A. Giese, H. A. Kretschmar, and P. Tavan. 2005. Molecular dynamics simulations indicate a possible role of parallel β-helices in seeded aggregation of poly-Gln. *Biophys. J.* 88:2442–2451.

28. Smith, A. V., and C. K. Hall. 2000. Bridging the gap between homopolymer and protein models: a discontinuous molecular dynamics study. *J. Chem. Phys.* 113:9331–9342.

29. Smith, A. V., and C. K. Hall. 2001. α-helix formation: discontinuous molecular dynamics on an intermediate resolution model. *Proteins.* 44:344–360.

30. Smith, A. V., and C. K. Hall. 2001. Assembly of a tetrameric α-helical bundle: computer simulations on an intermediate resolution protein model. *Proteins.* 44:376–391.

31. Smith, A. V., and C. K. Hall. 2001. Protein folding versus aggregation: computer simulations on an intermediate resolution protein model. *J. Mol. Biol.* 312:187–202.

32. Nguyen, H. D., A. J. Marchut, and C. K. Hall. 2004. Solvent effects on the conformational transition of a model polyalanine peptide. *Protein Sci.* 13:2909–2924.

33. Perutz, M. F. 1999. Glutamine repeats and neurodegenerative diseases: molecular aspects. *Trends Biochem. Sci.* 24:58–63.

34. Perutz, M. F., R. Staden, L. Moens, and I. D. Baere. 1993. Polar zippers. *Curr. Biol.* 3:249–253.

35. Perutz, M. F., T. Johnson, M. Suzuki, and J. T. Finch. 1994. Glutamine repeats as polar zippers: their possible role in inherited neurodegenerative diseases. *Proc. Natl. Acad. Sci. USA.* 91:5355–5358.

36. Perutz, M. 1994. Polar zippers: their role in human disease. *Protein Sci.* 3:1629–1637.

37. Bevivino, A. E., and P. J. Loll. 2001. An expanded glutamine repeat destabilizes native ataxin-3 structure and mediates formation of parallel β-fibrils. *Proc. Natl. Acad. Sci. USA.* 98:11955–11960.

38. Tanaka, M., I. Morishima, T. Akagi, T. Hashikawa, and N. Nukina. 2001. Intra- and intermolecular β-pleated sheet formation in glutamine-repeat inserted myoglobin as a model for polyglutamine diseases. *J. Biol. Chem.* 276:45470–45475.

39. Scherzinger, E., R. Lurz, M. Turmaine, L. Mangiarini, B. Hollenbach, R. Hasenbank, G. P. Bates, S. W. Davies, H. Lehrach, and E. E. Wanker. 1997. Huntingtin-encoded polyglutamine expansions form amyloid-like protein aggregates in vitro and in vivo. *Cell.* 90: 549–558.

40. Cooper, J. K., G. Schilling, M. F. Peters, W. J. Herring, A. H. Sharp, Z. Kaminsky, J. Masone, F. A. Khan, M. Delanoy, D. R. Borchelt, V. L. Dawson, T. M. Dawson, and C. A. Ross. 1998. Truncated N-terminal fragments of huntingtin with expanded glutamine repeats form nuclear and cytoplasmic aggregates in cell culture. *Hum. Mol. Genet.* 7:783–790.

41. Perutz, M. F., J. T. Finch, J. Berriman, and A. Lesk. 2002. Amyloid fibers are water-filled nanotubes. *Proc. Natl. Acad. Sci. USA.* 99:5591–5595.

42. Sikorski, P., and E. Atkins. 2005. New model for crystalline polyglutamine assemblies and their connection with amyloid fibrils. *Biomacromolecules.* 6:425–432.

43. Sunde, M., L. C. Serpell, M. Bartlam, P. E. Fraser, M. B. Pepys, and C. C. F. Blake. 1997. Common core structure of amyloid fibrils by synchrotron X-ray diffraction. *J. Mol. Biol.* 273:729–739.

44. Sharma, D., L. M. Shinchuk, H. Inouye, R. Wetzel, and D. A. Kirschner. 2005. Polyglutamine homopolymers having 8–45 residues form slablike β-crystallite assemblies. *Proteins.* 61:398–411.

45. Wacker, J. L., M. H. Zareie, H. Fong, M. Sarikaya, and P. J. Muchowski. 2004. Hsp70 and Hsp40 attenuate formation of spherical and annular polyglutamine oligomers by partitioning monomer. *Nat. Struct. Mol. Biol.* 11:1215–1222.

46. Lashuel, H. A., B. M. Petre, J. Wall, M. Simon, R. J. Nowak, T. Walz, and P. T. Lansbury Jr. 2002. α-synuclein, especially the Parkinson's disease-associated mutants, forms pore-like annular and tubular protofibrils. *J. Mol. Biol.* 322:1089–1102.

47. Ding, T. T., S.-J. Lee, J.-C. Rochet, J. Peter, and T. Lansbury. 2002. Annular α-synuclein protofibrils are produced when spherical protofibrils are incubated in solution or bound to brain-derived membranes. *Biochemistry.* 41:10209–10217.

48. Kimura, Y., S. Koitabashi, A. Kakizuka, and T. Fujita. 2001. Initial processo of polyglutamine aggregate formation in vivo. *Genes Cells.* 6:887–897.

49. Nguyen, H. D., and C. K. Hall. 2004. Molecular dynamics simulations of spontaneous fibril formation by random-coil peptides. *Proc. Natl. Acad. Sci. USA.* 101:16180–16185.

50. Nguyen, H. D., and C. K. Hall. 2004. Phase diagrams describing fibrillization by polyalanine peptides. *Biophys. J.* 87:4122–4134.

51. Nguyen, H. D., and C. K. Hall. 2005. Kinetics of fibril formation by polyalanine peptides. *J. Biol. Chem.* 280:9074–9082.

52. Takada, S., Z. Luthey-Schulten, and P. G. Wolynes. 1999. Folding dynamics with nonadditive forces: a simulation study of a designed helical protein and a random heteropolymer. *J. Chem. Phys.* 110:11616–11629.

53. Alder, B. J., and T. E. Wainwright. 1959. Studies in molecular dynamics. I. General method. *J. Chem. Phys.* 31:459–466.

54. Rapaport, D. C. 1979. Molecular dynamics study of a polymer chain. *J. Chem. Phys.* 71:3299–3303.

55. Bellemans, A., J. Orban, and D. V. Belle. 1980. Molecular dynamics of rigid and non-rigid necklaces of hard disks. *Mol. Phys.* 39:781–782.

56. Stickle, D. F., L. G. Presta, K. A. Dill, and G. D. Rose. 1992. Hydrogen bonding in globular proteins. *J. Mol. Biol.* 226:1143–1159.

57. Ding, F., J. M. Borreguero, S. V. Buldyrey, H. E. Stanley, and N. V. Dokholyan. 2003. Mechanism for the α-helix to β-hairpin transition. *Proteins.* 53:220–228.

58. Smith, S. W., B. D. Freeman, and C. K. Hall. 1997. Molecular dynamics for polymeric fluids using discontinuous potentials. *J. Comput. Phys.* 134:16–30.

59. Andersen, H. C. 1980. Molecular dynamics simulations at constant pressure and/or temperature. *J. Chem. Phys.* 72:2384–2393.

60. Chen, S., V. Berthelier, W. Yang, and R. Wetzel. 2001. Polyglutamine aggregation behavior in vitro supports a recruitment mechanism of cytotoxicity. *J. Mol. Biol.* 311:173–182.

61. Zhang, S., T. Holmes, C. Lockshin, and A. Rich. 1993. Spontaneous assembly of a self-complementary oligopeptide to form a stable macroscopic membrane. *Proc. Natl. Acad. Sci. USA.* 90:3334–3338.

62. Xiong, H., B. L. Buckwalter, H.-M. Shieh, and M. H. Hecht. 1995. Periodicity of polar and nonpolar amino acids is the major determinant of secondary structure in self-assembling oligomeric peptides. *Proc. Natl. Acad. Sci. USA.* 92:6349–6353.

63. Hartgerink, J. D., J. R. Granja, R. A. Milligan, and M. R. Ghadiri. 1996. Self-assembling peptide nanotubes. *J. Am. Chem. Soc.* 118:43–50.

64. Zhang, S., and M. Altman. 1999. Peptide self-assembly in functional polymer science and engineering. *React. Funct. Polym.* 41:91–102.(

65. Caplan, M. R., P. N. Moore, S. Zhang, R. D. Kamm, and D. A. Lauffenburger. 2000. Self-assembly of a β-sheet protein governed by relief of electrostatic replulsion relative to van der Waals attraction. *Biomacromolecules.* 1:627–631.

66. Holmes, T. C., S. de Lacalle, X. Su, G. Liu, A. Rich, and S. Zhang. 2000. Extensive neurite outgrowth and active synapse formation on self-assembling peptide scaffolds. *Proc. Natl. Acad. Sci. USA.* 97:6728–6733.

67. Aggeli, A., I. A. Nyrkova, M. Bell, R. Harding, L. Carrick, T. C. B. McLeish, A. N. Semenov, and N. Boden. 2001. Hierarchical self-assembly of chiral rod-like molecules as a model for peptide β-sheet tapes, ribbons, fibrils, and fibers. *Proc. Natl. Acad. Sci. USA.* 98: 11857–11862.

68. Fernandez-Lopez, S., H.-S. Kim, E. C. Choi, M. Delgado, J. R. Granja, A. Khasanov, K. Kraehenbuehl, G. Long, D. A. Weinberger, K. M. Wilcoxen, and M. R. Ghadiri. 2001. Antibacterial agents based on the cyclic D,L-α-peptide architecture. *Nature.* 412:452–455.

69. Zhang, S., D. M. Marini, W. Hwang, and S. Santoso. 2002. Design of nanostructured biological materials through self-assembly of peptides and proteins. *Curr. Opin. Chem. Biol.* 6:865–871.

70. Vauthey, S., S. Santoso, H. Gong, N. Watson, and S. Zhang. 2002. Molecular self-assembly of surfactant-like peptides to form nanotubes and nanovesicles. *Proc. Natl. Acad. Sci. USA.* 99:5355–5360.

71. Santoso, S., W. Hwang, H. Hartman, and S. Zhang. 2002. Self-assembly of surfactant-like peptides with variable glycine tails to form nanotubes and nanovesicles. *Nano Lett.* 2:687–691.

72. Marini, D. M., W. Hwang, D. A. Lauffenburger, S. Zhang, and R. D. Kamm. 2002. Left-handed helical ribbon intermediates in the self-assembly of a β-sheet peptide. *Nano Lett.* 2:295–299.

73. Scheibel, T., R. Parthasarathy, G. Sawicki, X.-M. Lin, and H. Jaeger. 2003. Conducting nanowires built by controlled self-assembly of amyloid fibers and selective metal deposition. *Proc. Natl. Acad. Sci. USA.* 100:4527–4532.